Optical fiber photoacoustic–photothermal probe

P. C. Beard, F. Pérennès, E. Draguioti, and T. N. Mills

Department of Medical Physics and Bioengineering, University College London, Shropshire House, 11-20 Capper Street, London WC1E 6JA, UK

Received May 29, 1998

We describe the operation of an all-optical probe that provides an alternative means of implementing photoacoustic and photothermal investigative techniques, particularly those used in biomedical applications. The probe is based on a transparent, acoustically and thermally sensitive Fabry–Perot polymer film sensor mounted at the end of an optical fiber. We demonstrate the ability of the system to make photoacoustic and photothermal measurements simultaneously and evaluate its photothermal response, using a nonscattering liquid target of known and adjustable absorption coefficient. The acoustic and thermal noise floors were 2 kPa and 6×10^{-3} °C, respectively, obtained over a 25-MHz measurement bandwidth and 30 signal averages. © 1998 Optical Society of America

OCIS codes: 110.5120, 350.5340, 000.1435.

Pulsed photoacoustic and photothermal techniques are investigative methods in which short subablation-threshold excitation laser pulses are absorbed in a target absorber, producing both acoustic (thermoelastic) and thermal waves. These waves act as carriers of information relating to the optical, acoustic, and thermal properties of the target absorber and can be used to describe its constituents and structure. Applications include the nondestructive testing of materials and structures[1] and the characterization of biological media.[2,3] Although photoacoustic and photothermal techniques provide an inherently powerful means of characterizing a target, their practical implementation can present difficulties. This is particularly true when it is required that (i) the generation and detection of the photoacoustic or photothermal signals take place on the same side of the target for reasons of limited access and (ii) the acoustic–thermal detector be placed close to or in contact with the target to avoid diffraction-induced distortion in the photoacoustic signal and low photothermal sensitivity owing to the rapid attenuation of thermal waves. The acoustic–thermal detector therefore has to be transparent (e.g., as in the method used in Ref. 4) so that it does not obstruct the excitation laser beam; this requirement excludes most conventional piezoelectric and pyroelectric contact transducer configurations. Radiometric detection can be used for same-side photothermal measurements[1] but has the disadvantages of relatively low temperature resolution (~0.1 °C) and, if optical fiber delivery is required, the need for use of special fibers.

In this Letter we describe an alternative method of implementing photoacoustic and photothermal techniques that can overcome the above limitations by the use of an all-optical probe based on an acoustically and thermally sensitive transparent Fabry–Perot polymer film sensor. The use of this type of probe for making photoacoustic measurements[5] and its ultrasonic acoustic response[6] were reported previously. In this Letter we demonstrate the ability of the system to make both photoacoustic and photothermal measurements simultaneously with high sensitivity and evaluate its photothermal response by using a nonscattering liquid absorber.

A schematic of the sensor head is shown in Fig. 1. A multimode optical fiber with a transparent Fabry–Perot polymer film sensor mounted at its distal end is placed in contact with the target absorber. Nanosecond, submillijoule optical pulses at a suitable wavelength are launched into the fiber, transmitted through the sensor, and absorbed in the target, producing thermal waves with a typical duration of the order of a few hundred milliseconds. In addition, rapid thermal expansion occurs, generating ultrasonic thermoelastic waves with a typical duration of several hundred nanoseconds. Both thermal and thermoelastic waves are detected by the sensor at the tip of the fiber. The sensor itself comprises a transparent 50-μm-thick polyethylene terepthalate (PET) film acting as a low-finesse Fabry–Perot interferometer, which is illuminated by light launched into the fiber from a cw low-power laser source. An incident thermal or thermoelastic wave changes the optical thickness of the film and hence the optical phase difference between the Fresnel reflections from the two sides of the film. This change produces a corresponding intensity modulation in the light reflected from the sensing film, which is then detected by a photodiode. Linear operation is achieved for small measurand-induced phase shifts by operation of the

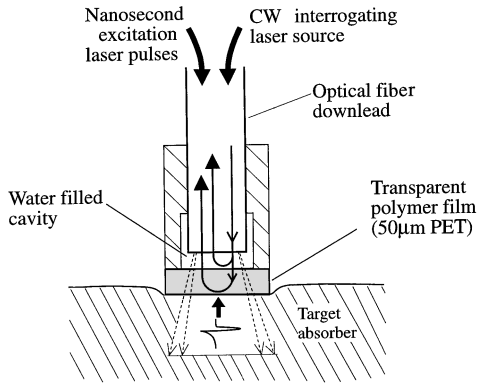

Fig. 1. Schematic of sensor head for generating and detecting photoacoustic and photothermal signals in a target absorber.

0146-9592/98/151235-03$15.00/0

interferometer at quadrature. The water cavity (Fig. 1) provides an acoustic and thermal impedance match to the fiber side of the sensing film. It also ensures that the Fresnel reflection coefficients on both sides of the film are the same (assuming that the refractive index of the target is close to that of water), resulting in high fringe visibility for optimum sensitivity.

Excitation laser pulses were provided by a frequency-doubled Q-switched Nd:YAG laser operating at 532 nm. The 633-nm cw output of a 6-mW He–Ne laser was used to interrogate the sensor. Both laser wavelengths were launched into a 10-m length of 380-μm-core all-silica optical fiber acting as the down-lead to the sensor head, which was placed in direct contact with the target absorber. Details of the sensor head design and the method of attaining quadrature based on exploiting variations in thickness across the area of the sensor film are described in Ref. 6. The signal-modulated cw 633-nm light reflected back from sensing film was detected by a 25-MHz silicon p–i–n photodiode, the output of which was displayed and signal averaged by a 500-MHz digitizing oscilloscope. To avoid obscuring the photoacoustic signal we removed repetitive optical and electrical noise from the Q-switched laser by subtracting a reference waveform containing only the noise.[5] The target absorber used was a nonscattering ink of known absorption coefficient μ_a.[7] This ink was diluted with an acidic buffer (Tris, pH 3) to yield a range of solutions of different values of μ_a. The incident fluence was 0.27 mJ/mm^2.

We obtained the acoustic system sensitivity by comparing the sensor output with a calibrated 25-MHz polyvinyl fluoride membrane hydrophone; it was 140 mV/MPa, with an acoustic noise floor of 2 kPa over a 25-MHz measurement bandwidth and 30 averages. We established the dc thermal system sensitivity by placing the sensor head in a water bath and recording the sensor output as the temperature was varied. A calibrated thermocouple placed immediately adjacent to the sensor head was used as a reference. The dc thermal system's sensitivity was 32 mV/°C, with a thermal noise floor of 6.3×10^{-3} °C, also over a 25-MHz measurement bandwidth and 30 averages. By varying the temperature over 25 °C we could observe a maximum and a minimum of the interferometer transfer function (indicating a phase shift of π rad), giving a temperature (phase) sensitivity of 0.13 rad/°C.

Figure 2 demonstrates the dual sensing ability of the system, showing the photoacoustic and photothermal signals generated in an ink–Tris solution of absorption coefficient $\mu_a = 70$ cm^{-1} over several time scales. Figure 2(a) shows the short-duration (400-ns) photoacoustic signals; it is assumed that the sensor gives an accurate representation of them because of its wideband (20-MHz) uniform acoustic frequency response.[6] The initial thermoelastic wave X (peak acoustic pressure, 80 kPa) is that generated immediately adjacent to the sensing film by the absorption of the Q-switched laser pulse, whereas the second, much smaller amplitude thermoelastic wave Y is the time-delayed reflection of X from the tip of the optical fiber. The step decrease immediately following the initial thermoelastic wave X is due to the initial heating of the target by the laser pulse and can be regarded as the onset of the rising edge of the thermal wave. This slow increase in the thermal signal can be seen more clearly in Fig. 2(b), which shows Fig. 2(a) over a longer time scale. The full photothermal signal is shown in Fig. 2(c): the thermoelastic waves cannot be seen on this time basis because of the relatively long sampling interval of the digitizing oscilloscope.

To examine the thermal response of the sensor we generated photothermal signals in ink–Tris solutions of different values of μ_a, as shown in Fig. 3. These signals are inverted compared with those in Fig. 2, so increasing temperature is now represented by a positive sensor output. For $\mu_a = 70$ cm^{-1}, the peak temperature increase of the photothermal signal, as determined from the measured dc thermal sensitivity, is 0.23 °C. Assuming that all the laser energy is absorbed and converted to heat and taking the density and the specific heat capacity of the ink absorber to be those of water, the calculated peak temperature (using simple calorimetry) is a factor of 2 higher at 0.45 °C. The discrepancy arises from the fact that the dc thermal sensitivity was obtained under steady-state conditions in which the temperature across the sensor film was constant. The photothermal wave, however, has a short wavelength, resulting in a significant temperature gradient across the film; i.e., the sensor film is thermally thick. Thus, because the sensor output represents the integral of the temperature distribution across the film, the use of the dc thermal sensitivity calibration causes the peak temperature to be underestimated.

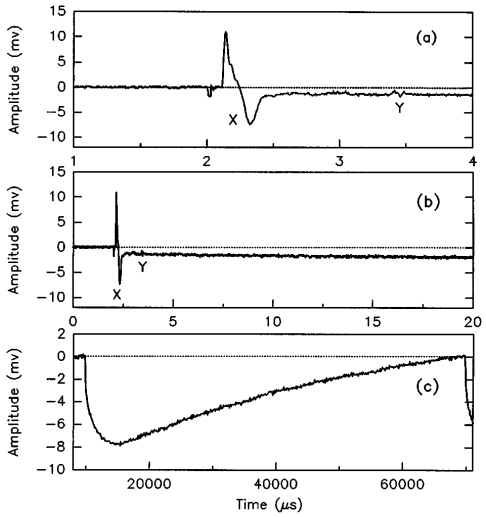

Fig. 2. Sensor output in response to photoacoustic and photothermal signals generated in an ink–Tris absorber ($\mu_a = 70$ cm^{-1}) over different time scales. (a) Photoacoustic signals. X is the initial thermoelastic wave generated immediately adjacent to the sensing film, and Y is the reflection of X from the fiber tip. (b) Increased time scale of (a), showing the photoacoustic signal and onset of the rise of the thermal wave. (c) Expanded time scale, showing the complete thermal wave. Fluence, 0.27 mJ/mm^2; pulse duration, 5 ns; repetition rate, 16 Hz; signals averaged over 30 shots.

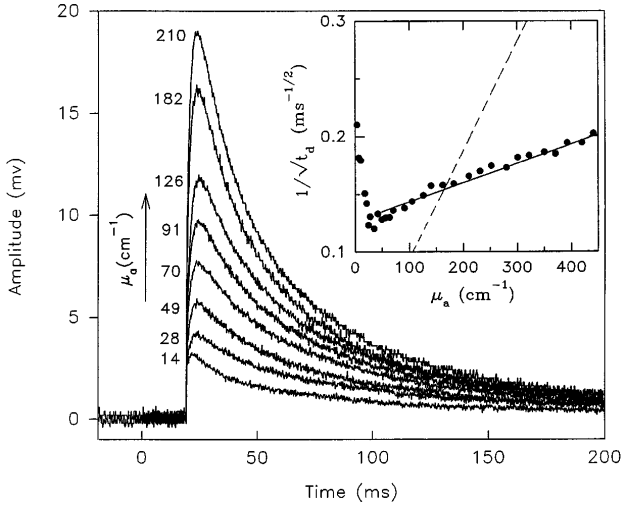

Fig. 3. Photothermal signals generated in an ink–Tris absorber for different optical absorption coefficients μ_a. Inset, relationship between $1/\sqrt{t_d}$ (where t_d is the $1/e$ photothermal decay time) and μ_a: the dashed line represents predicted relationship. Fluence, 0.27 mJ/mm^2; pulse duration, 5 ns; repetition rate, 2 Hz; signals averaged over 30 shots.

The thermally thick nature of the sensing film also manifests itself in the relationship between the decay time t_d of the photothermal signals (the time taken for the signal to fall to $1/e$ of its maximum value) and the absorption coefficient μ_a; the former is an important parameter in photothermal characterization techniques. Assuming that the sensor measures the temperature at the boundary between the sensing film and the ink absorber, an approximation to t_d can be found by the approach taken by McKenzie[8] to derive thermal time constants for one-dimensional heat flow such that

$$t_d = 1.6/\mu_a{}^2 D\,, \tag{1}$$

where D is the thermal diffusivity of the absorber (taken to be that of water for the ink–Tris absorber). Plotting $1/\sqrt{t_d}$ as a function of μ_a as in Fig. 3 therefore linearizes Eq. (1). For μ_a between 50 and 450 cm^{-1}, the experimentally measured decay times obey the inverse square relationship of Eq. (1). The slope, however, is a factor of 5 less than Eq. (1) would suggest because of the band-limiting effect of the thermally thick sensing film, which reduces the change in t_d with μ_a. The practical significance of this reduction is that the ability of the system to detect changes in μ_a is reduced and hence so is its photothermal diagnostic ability. A solution to this problem would be to reduce the film thickness so that it is small compared with the characteristic thermal wavelength. Note also that for μ_a between 50 and 450 cm^{-1} the straight line plotted through the experimental data has a nonzero Y intercept; i.e., the absolute values of the decay times are shorter than expected by a μ_a-independent amount. This result indicates the influence of radial heat flow, which, for $1/\mu_a \ll d$ [where d is the diameter of the laser spot (=0.53 mm)], is independent of μ_a to a first approximation. Once $1/\mu_a$ begins to approach d, radial heat flow appears to become critically dependent on μ_a, as shown in Fig. 3, where the decay times begin to fall very rapidly ($1/\sqrt{t_d}$ increases) with decreasing μ_a for $\mu_a < 50$ cm^{-1}. The high sensitivity of t_d to changes in μ_a in this region could perhaps be exploited for making measurements in targets of low absorption. One could choose to operate in this region, for a given range of μ_a, by suitable choice of the illuminating spot size, either by selection of the fiber core diameter or by altering the fiber-sensing film separation.

An all-optical probe that can generate and detect photoacoustic and photothermal transients simultaneously has been demonstrated. A level of acoustic and thermal sensitivity has been achieved that is comparable with those of conventional piezoelectric, pyroelectric, and radiometric detection methods. The photothermal temporal response of the sensor is influenced by the thickness of the sensing film and by radial heat flow: Reducing the film thickness and optimizing the source diameter would enable the photothermal diagnostic ability to be improved yet further. There is considerable potential for miniaturization by dispensing with the sensor head and bonding the sensing film directly to the tip of the fiber. This would make the system suited to biomedical applications that require an electrically passive, miniature flexible probe-type configuration for their implementation. One such area that we are currently investigating is the intravascular photoacoustic–photothermal characterization of arterial tissue.[7,9]

This research was supported by the British Heart Foundation.

References

1. R. E. Imhoff, B. Zhang, and D. J. S. Birch, in *Non-Destructive Evaluation: Progress in Photothermal and Photoacoustic Science and Technology,* A. Mandelis, ed. (Prentice-Hall, Englewood Cliffs, N.J., 1994), Vol. 2, pp. 185–236.
2. A. A. Oraevsky, S. L. Jacques, and F. Tittel, Appl. Opt. **36,** 402 (1997).
3. S. A. Prahl, I. A. Vitkin, B. Bruggemann, B. C. Wilson, and R. R. Anderson, Phys. Med. Biol. **37,** 1203 (1992).
4. G. Paltauf and H. Schmidt-Kloiber, J. Appl. Phys. **82,** 1525 (1997).
5. P. C. Beard and T. N. Mills, Proc. SPIE **2388,** 446 (1995).
6. P. C. Beard and T. N. Mills, Appl. Opt. **35,** 663 (1996).
7. P. C. Beard and T. N. Mills, Phys. Med. Biol. **42,** 177 (1997).
8. A. L. McKenzie, Phys. Med. Biol. **31,** 967 (1986).
9. F. Pérennès, P. C. Beard, and T. N. Mills, in *Horizons de l'Optique 1997* (Société Française d'Optique, Orsay Cedex, France, 1997), p. A-13.